Helium atom diffraction measurements of the surface structure and vibrational dynamics of CH_3–Si(111) and CD_3–Si(111) surfaces

James S. Becker,[1] Ryan D. Brown,[1] Erik Johansson,[2] Nathan S. Lewis,[2] and S. J. Sibener[1,a)]

[1]*Department of Chemistry and The James Franck Institute, The University of Chicago, 929 E. 57th Street, Chicago, Illinois 60637, USA*

[2]*Beckman Institute and Kavli Nanoscience Institute, Division of Chemistry and Chemical Engineering, 210 Noyes Laboratory, 127-72, California Institute of Technology, Pasadena, California 91125, USA*

(Received 13 July 2010; accepted 5 August 2010; published online 13 September 2010)

The surface structure and vibrational dynamics of CH_3–Si(111) and CD_3–Si(111) surfaces were measured using helium atom scattering. The elastic diffraction patterns exhibited a lattice constant of 3.82 Å, in accordance with the spacing of the silicon underlayer. The excellent quality of the observed diffraction patterns, along with minimal diffuse background, indicated a high degree of long-range ordering and a low defect density for this interface. The vibrational dynamics were investigated by measurement of the Debye–Waller attenuation of the elastic diffraction peaks as the surface temperature was increased. The angular dependence of the specular ($\theta_i = \theta_f$) decay revealed perpendicular mean-square displacements of 1.0×10^{-5} Å^2 K^{-1} for the CH_3–Si(111) surface and 1.2×10^{-5} Å^2 K^{-1} for the CD_3–Si(111) surface, and a He-surface attractive well depth of ~7 meV. The effective surface Debye temperatures were calculated to be 983 K for the CH_3–Si(111) surface and 824 K for the CD_3–Si(111) surface. These relatively large Debye temperatures suggest that collisional energy accommodation at the surface occurs primarily through the Si–C local molecular modes. The parallel mean-square displacements were 7.1×10^{-4} and 7.2×10^{-4} Å^2 K^{-1} for the CH_3–Si(111) and CD_3–Si(111) surfaces, respectively. The observed increase in thermal motion is consistent with the interaction between the helium atoms and Si–CH_3 bending modes. These experiments have thus yielded detailed information on the dynamical properties of these robust and technologically interesting semiconductor interfaces. © *2010 American Institute of Physics*. [doi:10.1063/1.3483465]

I. INTRODUCTION

Surface functionalization is a powerful method for tailoring the physical and chemical properties of interfaces. Several synthetic routes have allowed the fabrication of high-coverage atomic and molecular layers on a variety of metallic and semiconducting surfaces,[1–5] with self-assembled monolayers (SAMs) produced by thiol linkages to Au(111) comprising the most ubiquitous and advanced methodology.[2,6–15] Such SAMs have evolved into a sophisticated technology with applications in nanoscience and biotechnology.[16–19] With the success of the SAM/Au system, strategies for creating molecular layers on semiconductor substrates have been the focus of ongoing research. Reactive additions to the Si(100) and Si(111) surfaces have emerged as an effective method for the functionalization of semiconductor interfaces.[4,20–23]

Hydrogen-terminated Si(111) surfaces are attractive substrates because they can be fabricated with large, atomically flat terraces.[24] Unfortunately, a major drawback of the H-terminated surface is that it rapidly oxidizes upon exposure to the ambient environment.[25] To protect and insulate the surface, the H–Si(111) surface can be alkylated with Grignard reagents to create an inert surface that maintains the desirable interfacial electrical properties of the H–Si(111) surface.[3,26,27] Specifically, methyl-terminated Si(111) surfaces offer a particularly robust and durable semiconductor interface for use in devices such as photodiodes and Schottky junctions.[28,29] The two-step halogenation/Grignard methylation method generates surfaces that have nearly complete coverage (>95%) and large, atomically flat terraces.[30] Methyl termination electrically and chemically passivates the silicon surface and, in particular, provides resistance against surface oxidation and thermal degradation. The methyl-terminated surface has been shown to be stable in air for extended periods (>600 hr) and to be unaffected by extreme temperatures (~700 K).[31,32]

CH_3-terminated Si(111) has been characterized by a variety of standard surface science techniques to determine the surface's structural, vibrational, and electronic properties. A combination of low-energy electron diffraction (LEED) and cryogenic scanning tunneling microscopy (STM) measurements have revealed that methyl termination creates a (1 × 1) surface with a methyl-methyl spacing of 3.8 Å.[30,33,34] The vibrational spectra of the CH_3–Si(111) surface have been measured by transmission infrared spectroscopy (TIRS) and by high-resolution electron energy loss spectroscopy (HREELS), allowing the assignment of the vibrational modes of this interface.[34–36] These spectroscopic techniques

a)Author to whom correspondence should be addressed. Electronic mail: s-sibener@uchicago.edu.

have provided functional group analysis and a detailed picture of the Si–C covalent bonding. A photoelectron spectroscopic study has shown that methylation creates a surface dipole, slightly shifting the silicon valence and conduction band edges at the surface.[32,33] Furthermore, the low levels of midgap states measured by scanning tunneling spectroscopy attest to the high degree of electrical passivation that is provided by methyl termination.[37] To date, although the static properties of such surfaces have been studied rather thoroughly, the dynamical properties of such systems remain largely unexplored. An understanding of the vibrational dynamics can provide insight into energy accommodation, vibrational decay pathways, and heat flow at the surface.

We describe herein a helium atom scattering (HAS) study that has revealed static and dynamical properties of the methyl-terminated Si(111) surface that are inaccessible by other techniques. HAS provides a nondestructive neutral atom probe of structure and low-energy vibrations, with unique surface sensitivity. In this work, helium atom diffraction was employed to examine the surface structure, gas-surface interaction potentials, and interfacial vibrational dynamics of CH_3- and CD_3-terminated Si(111). The surface lattice constant and average domain size of such systems was determined by analysis of the helium diffraction patterns. In addition, the thermal motion at the interface was quantified by extracting the temperature-dependent mean-square displacements perpendicular to and parallel to the surface. Using the angular dependence of the Debye–Waller factor, the helium-surface well depth and surface Debye temperatures were calculated for CH_3- and CD_3-terminated Si(111) surfaces.

II. MATERIALS AND EXPERIMENTAL METHODS

The Si(111) wafers were double-side polished, float-zone grown, and had a resistivity of 63–77 Ω cm (Silicon Quest International, Santa Clara, CA). Water was obtained from a Barnstead Nanopure system (Waltham, MA) and had a resistivity of 18.3 MΩ cm.

Si(111) surfaces were functionalized by a two-step chlorination/alkylation method.[26] Briefly, Si wafers were cut into (1 cm × 3 cm) rectangles. Contaminants were removed from the wafer-surface by sequential rinsing with water, methanol, acetone, methanol, and finally water. Without allowing the wafer to dry, the sample was transferred to a test-tube that contained freshly prepared Piranha solution [H_2SO_4 (97 wt %): H_2O_2 (29–32 wt %)), 3:1 by volume]. The solution was then heated to 100 °C for 5 min, after which the wafer was allowed to cool slowly to ambient temperature followed by a rinse with copious amounts of water.

The cleaned samples were then immersed into 6 M HF(aq) [prepared by dilution of 49% HF(aq) (semiconductor grade, Transene Co., Inc., Danvers, MA)] for 45 s, rinsed with water, and transferred to an Ar-purged solution of 11 M NH_4F(aq) (semiconductor grade, Transene Co., Inc., Danvers, MA). The NH_4F(aq) was continuously purged with Ar for the duration of the etching (10 min) and the samples were agitated periodically to prevent bubbles from adhering to the sample. This procedure is known to produce atomically flat, H-terminated Si(111) surfaces.[36,38] After etching, the samples were transferred to an N_2-purged glove-box that contained less than 10 ppm of O_2.

Cl–Si(111) surfaces were prepared by transferring H–Si(111) samples to test tubes that contained saturated solutions of PCl_5 (99.998% metal basis, Alfa Aesar, Ward Hill, MA) in chlorobenzene (anhydrous, 99.8%, Sigma Aldrich, St. Louis, MO) to which a small amount of radical initiator (benzoyl peroxide, Aldrich reagent grade, 97%, Sigma Aldrich) had been added. The samples were heated to 90–95 °C for 45 min, after which they were rinsed with chlorobenzene and then with tetrahydrofuran (THF).

Directly following the chlorination, to prepare CH_3–Si(111) surfaces, the samples were transferred into a 1.0 M solution of CH_3MgCl in THF (Sigma Aldrich) and heated to 70 °C for 3 h. To prepare CD_3–Si(111) surfaces, the samples were transferred into a 3.0 M solution of CD_3MgI in diethyl ether (Sigma Aldrich) and kept at room temperature for 48 h. Following alkylation, the samples were rinsed with copious amounts of THF or diethyl ether, after which the Si surfaces were placed in anhydrous methanol, removed from the glove-box, and sonicated for 5 min each in methanol, acetonitrile, and water. The success of the alkylation reaction was monitored via x-ray photoelectron spectroscopy, which confirmed that the Si atop sites had been fully terminated by Si–C bonds, and indicated that the level of surface oxidation was consistently well below 0.2 ML of SiO_2.[39]

For transport from Pasadena, CA to Chicago, IL, the samples were sealed in plastic containers under an inert atmosphere (less than 0.2 ppm O_2, 0.5 ppm H_2O) to effect minimal sample degradation.

A helium atom scattering apparatus with high energy-resolution and momentum-resolution was used to measure the surface structure and dynamics of methylated Si(111). The apparatus has been described in detail elsewhere.[40] Briefly, helium was expanded through a 20 μm nozzle source that was cooled by a closed-cycle helium refrigerator to generate a nearly monochromatic ($\Delta v/v \leq 1\%$) supersonic neutral atom beam. Primarily, a 46 meV beam (wave vector, $k_i = 9.4$ Å^{-1}; nozzle temperature, $T_n \sim 213$ K) was used for the experiments, while a 17.5 meV beam ($k_i = 5.73$ Å^{-1} and $T_n \sim 81$ K) was employed for measurements of the specular angular width. A mechanical chopper modulated the helium beam with a 50% duty cycle prior to collision. The beam was collimated to 0.22° [full width at half maximum (FWHM)] and impinged on the crystal (chopper-crystal distance =0.5473 m) that was housed in an ultrahigh vacuum surface-scattering chamber. The crystal was mounted on a six-axis manipulator that could be positioned precisely to control the incident angle θ_i, the azimuth ϕ, and the tilt χ, with respect to the scattering plane. Sample temperatures ranging from 30 to 900 K were achieved by tethering a heatable crystal mount to a closed-cycle helium refrigerator. Atoms were reflected into a triply differentially pumped rotatable detector with an overall instrument resolution of 0.5° (FWHM) and were ionized by electron bombardment

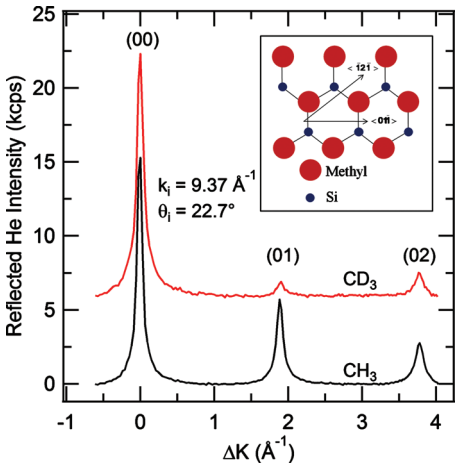

FIG. 1. Helium diffraction scans for the CH_3–Si(111) (black) and CD_3–Si(111) (red) surfaces showing first-order and second-order peaks. The inset is a schematic of the real space lattice.

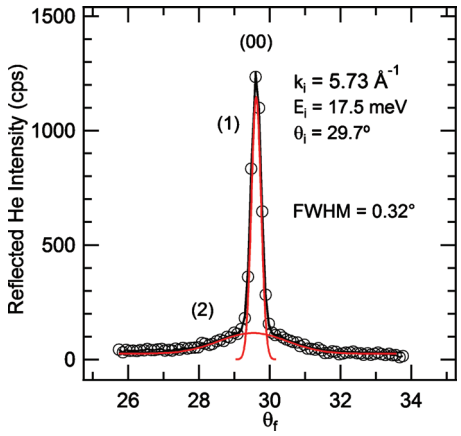

FIG. 2. Specular peak width analysis for the CH_3-terminated surface. The solid red lines are the fits to the coherent elastic peak (1) and the broad diffuse elastic/multiphonon background (2). The solid black line is the overall fit to the data (open circles). The full width half maximum of the narrow coherent elastic peak (1) is 0.32°.

(crystal-ionizer distance=0.5470 m). A quadrupole filter mass-selected the helium ions, which were then collected by an electron multiplier.

At the start of each experiment, the crystal was briefly heated to 700 K to remove any accumulated adsorbates and hydrocarbon contaminants.[32,34] Previous works have demonstrated that the methyl surface moieties are stable at these temperatures, which the highly sensitive helium reflectivity measurements performed herein have confirmed. Diffraction patterns were recorded by aligning the crystal at a given incident angle θ_i and a computer-controlled motor was used to scan the detector through the final angle θ_f. Typically, a beam energy of 46 meV (k_i=9.4 Å^{-1} and T_n=213 K) was used, so that the diffraction peaks were observable over the full angular range of the instrument. The thermal attenuation of the elastic scattering signal was recorded over a surface temperature T_S range of 200–500 K in 50 K steps. Specular, first-order, and second-order diffraction peaks were collected for each sample.

III. RESULTS AND DISCUSSION

Methyl termination of the Si(111) surface preserves the hexagonal unit cell native to the (111) crystal face.[30,33] Consistently, LEED patterns of such systems exhibit threefold symmetry with a hexagonal arrangement of the adlattice and a methyl group spacing of about 4 Å. Cryogenic STM measurements have shown the methyl-methyl separation to be 3.8 Å, which matches the spacing of the silicon underlayer. Elastic helium atom scattering provides a powerful method for determination of the surface structure and the coherence length of the surface. The beam used in this work illuminates a spot of approximately 3.7 mm in diameter, providing a macroscopic sampling of the surface. The scattering experiment is thus complementary to the local-scale structural measurements obtained by STM.

Figure 1 shows diffraction patterns collected from the CH_3-terminated (black) and CD_3-terminated (red) Si(111) surfaces at T_S=200 K, plotting the scattered helium intensity versus the parallel wave vector. The two diffraction patterns have been vertically offset for clarity. The incident angle was 22.7° and the azimuth was aligned along the $\langle \bar{1}2\bar{1} \rangle$ direction. The bottom axis has been transformed from the final angle θ_f to the parallel momentum transfer ΔK, using the equation

$$\Delta K = k_i(\sin(\theta_f) - \sin(\theta_i)). \tag{1}$$

The condition for elastic diffraction is met when

$$\Delta K = h\vec{b}_1 + k\vec{b}_2, \tag{2}$$

where h and k are the diffraction indices and b_i are the reciprocal lattice vectors. Both diffraction scans were recorded in the same geometry and showed two peaks spaced equivalently from the specular reflection (ΔK=0 Å^{-1}). These diffraction peaks appeared at ΔK=1.90 and 3.80 Å^{-1}, corresponding to a lattice constant of 3.82 Å for both the CH_3- and CD_3-terminated Si(111) surfaces. Helium diffraction thus revealed that the terminal methyl groups have the same spacing as the native Si(111), forming a (1×1) structure. Minimal diffuse background further indicated long-range order and low defect density across the crystal surface.[41]

The angular width of the specular peak was also analyzed to gain insight into the average coherence length of the surface (Fig. 2).[42,43] The surface is composed of large atomically flat terraces separated by single atom steps and the size of these terraces is approximately the coherence length. The measured specular width $\Delta\theta_{\text{exp}}$ is a convolution of the instrument function broadening $\Delta\theta_{\text{inst}}$ and the domain size broadening $\Delta\theta_w$, as given by

$$\Delta\theta_w^2 = \Delta\theta_{\text{exp}}^2 - \Delta\theta_{\text{inst}}^2. \tag{3}$$

The coherence length l_c can then be determined using[43]

$$l_c = \frac{5.54}{\Delta\theta_w k_i \cos(\theta_f)}. \tag{4}$$

For the purpose of this measurement, the neutral flight path from chopper to ionizer was lengthened to 1.549 m by addition of a cylindrical spacer to the detector. The additional length of the detector narrowed the acceptance angle to 0.29° (~0.02 Å^{-1}), thereby improving the overall angular resolution. Furthermore, the beam energy was lowered to 17.5

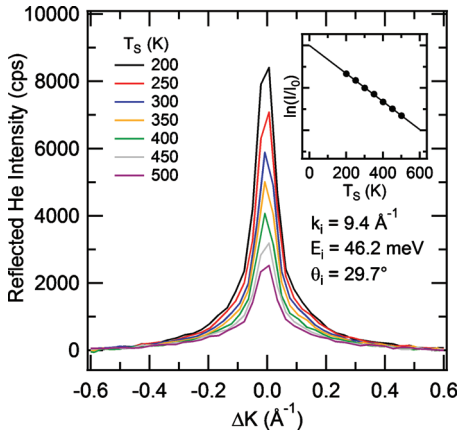

FIG. 3. Plot of the specular decay with surface temperature for CH_3–Si(111). The inset demonstrates that the decay is linear over the experimental temperature range.

meV (k_i=5.73 Å^{-1} and $T_n \sim 81$ K) to minimize the diffuse elastic and multiphonon contributions to the linewidth. These experimental parameters yield a maximum measurable domain size of about 900 Å. The peak in Fig. 2 was fit with two Gaussian functions to account for the narrow coherent elastic contribution (1) and for the broad diffuse elastic/multiphonon contribution (2). A FWHM of $\Delta\theta_{\text{exp}}=0.32°$ was determined from the fitting procedure. The higher resolution measurements showed the average domain size of the CH_3–Si(111) surface to be approximately 500 Å as calculated from Eq. (4). The domain size measured in the scattering experiment roughly agrees with the 200×200 nm STM images obtained previously.[30]

The thermal attenuation of the diffraction peaks provides atomic level insight into the surface vibrational dynamics.[44,45] The decay of the peak intensity with increasing surface temperature (Fig. 3) occurs through the increasing vibrational amplitude of the surface oscillators. The vibrational amplitude is quantified by measurement of the peak decay with T_S, and by calculation of the Debye–Waller factors. The mean-square displacements (MSD) of the methyl groups both perpendicular and parallel to the surface were then extracted from the Debye–Waller factor. The Debye–Waller argument states that elastic scattering decays exponentially with temperature, as given by

$$I = I_0 e^{-2W(T_S)}, \tag{5}$$

where I_0 is the peak intensity at T_S=0 K and $\exp[-2W(T_S)]$ is the Debye–Waller factor. The Debye–Waller factor contains contributions from perpendicular (Δk_z) and parallel (ΔK) components of momentum transfer and their associated mean-square displacements as given by

$$2W = \Delta k_z^2 \langle u_z^2 \rangle + \Delta K^2 \langle u_\parallel^2 \rangle. \tag{6}$$

ΔK is given in Eq. (1) and the expression for Δk_z is given by Eq. (7)

$$\Delta k_z = k_i \left\{ \left[\cos^2(\theta_f) + \frac{D}{E_i} \right]^{1/2} + \left[\cos^2(\theta_i) + \frac{D}{E_i} \right]^{1/2} \right\}, \tag{7}$$

where E_i is the incident beam energy and D is the He-surface attractive potential well depth, which in this expression accounts for the added acceleration of the helium atom before collision with the surface.[46]

The decay of the specular diffraction peak intensity was measured as a function of T_S. Assuming that the Debye model holds across the experimental temperature range (200–500 K), the mean-square displacements of the surface oscillators should increase linearly with surface temperature. Figure 3 displays the specular ($\Delta K=0$ Å^{-1}) peak decay produced by heating methyl-terminated Si(111) from 200 to 500 K in steps of 50 K. Data were collected with an incident beam energy E_i=46 meV (k_i=9.4 Å^{-1}) at $\theta_i=\theta_f=29.7°$. The inset shows the logarithm of the numerical peak integrals as a function of the surface temperature. A linear decay was observed for the system over the experimental range, consistent with the Debye model. The temperature coefficient of the perpendicular mean-square displacement was extracted from the thermal decay and, for simplicity, will be called the perpendicular MSD.

Equation (6) can be modified to include the temperature dependence of the Debye–Waller exponent

$$\sigma_{ijk} \equiv -\frac{d(2W)}{dT_S} = -\left[\Delta k_z^2 \frac{d\langle u_z^2 \rangle}{dT_S} + \Delta K^2 \frac{d\langle u_\parallel^2 \rangle}{dT_S} \right]. \tag{8}$$

The variable σ indicates the decay rate with the first index, either H or D, specifying CH_3 or CD_3 termination, and the last two indices designating the specific diffraction peak. For example, σ_{H00} symbolizes the specular peak decay for the methyl-terminated surface. Cooling experiments were also performed, and no thermal hysteresis was observed for either CH_3–Si(111) or CD_3–Si(111) systems. The presented data were collected by heating the crystals in 50 K increments.

To accurately quantify the perpendicular mean-square displacements, the normal component of momentum transfer must be fully characterized. As shown in Eq. (7), the perpendicular momentum transfer depends on $\cos^2\theta_i$ and on the well depth D, which is unknown for this system. For the specular geometry ($\theta_i=\theta_f$), Eq. (7) reduces to

$$\Delta k_z^2 = 4k_i^2 \left[\cos^2(\theta_i) + \frac{D}{E_i} \right]. \tag{9}$$

Figure 4 displays the specular decay for the methyl-terminated surface in (a) and for the CD_3-terminated surface in (b). The data were recorded with a 46 meV beam at incident angles of 36.2° (black circles), 29.7° (red squares), and 22.7° (blue diamonds). The specular decay rates can be linearized with respect to $\cos^2\theta_i$, as given by

$$\sigma_{00} = -a\cos^2(\theta_i) - b,$$

$$a = 4k_i^2 \frac{d\langle u_z^2 \rangle}{dT_S}, \tag{10}$$

$$b = a\frac{D}{E_i}.$$

A fit of the data provided the perpendicular mean-square displacement from the slope and the well depth from the intercept. In Fig. 5, σ_{H00} and σ_{D00} are shown in black circles and red squares, respectively, with the error bars representing

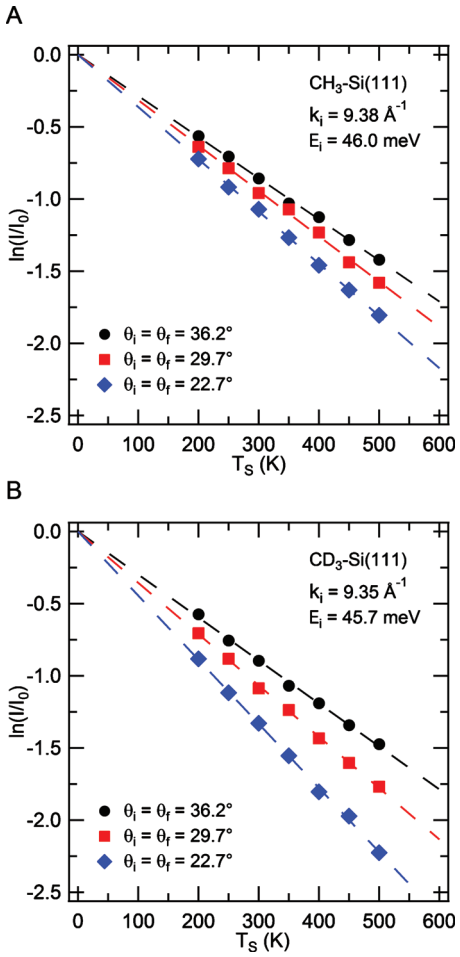

FIG. 4. Specular decay at three different incident angles for the (a) CH_3 and(b) CD_3 surfaces. The dashed lines are fits to the data and provide the decay rate σ.

the standard deviations calculated from independent measurements of each point. Linear fits to the specular data yielded a slope of -0.0035 and intercept of -0.00058 for CH_3–Si(111) surface and a slope of -0.0042 and intercept of -0.00055 for the CD_3–Si(111) surface. Taking $k_i = 9.38$ Å^{-1}, the perpendicular mean-square displacements were $(1.0 \pm 0.1) \times 10^{-5}$ and $(1.2 \pm 0.2) \times 10^{-5}$ Å^2 K^{-1} for the

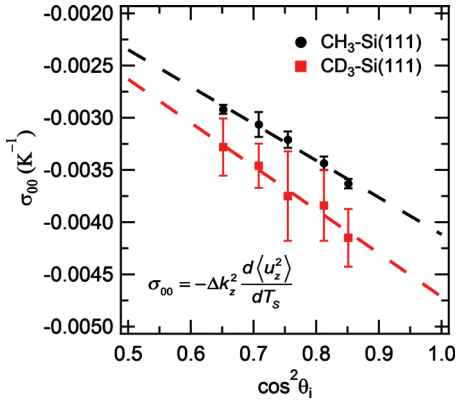

FIG. 5. Linear fits to the angular dependence of the Debye–Waller factor for CH_3–Si(111) (black circles) and CD_3–Si(111) (red squares). The slopes and intercepts characterize the perpendicular mean-square displacements and the well depths, respectively.

CH_3–Si(111) and CD_3–Si(111) surfaces, respectively. The CD_3–Si(111) surface exhibited a perpendicular MSD that was about 20% greater than the CH_3–Si(111) surface as expected from the isotopic substitution. The well depths determined from the intercepts were $D_H = 7.5 \pm 2.6$ meV and $D_D = 6.0 \pm 3.9$ meV, which are in agreement with other methyl-terminated systems.[7,47] We note that the well depths are equal within the precision of the measurement, as expected, since isotopic substitution does not alter the He-surface attractive potential. In subsequent sections, unless otherwise stated we will use the experimentally determined values of the well depth, noting that the use of the average value of 6.75 meV changes the results of our calculations by less than 5%.

A thorough discussion of the mean-square displacements requires the use of information on the CH_3–Si(111) normal modes and their respective vibrational frequencies, as determined by TIRS and HREELS. The methyl-Si group contains four vibrational modes: the C–Si stretching mode, the C–Si bending mode, the CH_3 rocking mode, and the C–Si rotational mode. The stretching and bending modes have been measured by HREELS to have frequencies of 678 and 507 cm^{-1}, respectively. The rocking mode has been measured by both techniques, with frequencies observed at 757 cm^{-1} by TIRS and at 789 cm^{-1} by HREELS. Finally, the rotational mode has not been observed but is expected from gas-phase spectra of methylsilane to have an excitation energy of about 200 cm^{-1} and a rotational barrier of $\sim$590 cm^{-1}.[48] To our knowledge, the spectrum of the CD_3-terminated surface has not been recorded, but the additional mass is expected to lower the vibrational frequencies based on gas-phase spectroscopy of isotopically substituted methylsilanes.[49]

The perpendicular mean-square displacements arise from vibrational motion normal to the crystal surface. A useful first comparison can be made with the Si(111)–(7×7) reconstructed surface.[50] By extrapolation, the perpendicular mean-square displacement from this surface is $\sim 2 \times 10^{-5}$ Å^2 K^{-1}, about double the value for the methyl-terminated Si(111) reported herein. In the harmonic limit of the Debye model, the MSD is proportional to the inverse of mass and to the inverse square of the Debye temperature θ_D.[44] The reduction in MSD can thus be attributed to a decrease of the effective surface mass from 28 to 15 amu and to an increase in the effective Debye temperature. The contribution from a change in the surface Debye temperature is discussed below.

A comparison of these data to the properties of other surfaces that have methyl termination can elucidate the most important vibrational modes associated with the measured Debye–Waller factors. For example, a methyl-terminated organic crystal, guanidinium methanesulfonate, investigated by Scoles and co-workers[47,51] showed a perpendicular MSD of about 3×10^{-4} Å^2 K^{-1}. The difference between the methyl-terminated Si(111) and the organic crystal stems from the type of motion involved in each system. The perpendicular surface motion for the organic crystal is a low-energy mode involving a shear vertical motion of the entire guanidinium sulfonate sheet. The perpendicular MSDs of various chain

length SAMs have been measured[7,13,52] and the thermal motion in the z-direction of such systems is about an order of magnitude greater than for CH_3-terminated Si(111), even though both systems project terminal methyl groups. For alkanethiol SAMs, low-energy librational modes of the whole chain are the primary contributors to the measured mean-square displacements. Hence, the stiffness of the methyl-terminated Si(111) arises from the rigidity of the directional, sp^3-hybrid Si–C covalent bonding in such systems.

Helium-surface attractive potential well depths can be estimated from the plethora of examples available for surfaces that are similar to methyl-terminated Si(111). The two experimental values determined herein are not statistically different from each other due to the large uncertainty in this type of indirect measurement. Bound-state resonances are a more precise method for evaluating the well depths, and the next two examples were measured using that technique.[53] Using helium scattering from a hydrogen-terminated Si(111) surface, Allison and co-workers[54] determined the attractive well depth to be 7.5 meV. The well depth of the methyl-terminated organic crystal was found to be 6.7 meV.[47] Well depths for a variety of alkanethiol self-assembled monolayers that possess terminal methyl groups have been calculated and the results range from 6.8 to 8.1 meV depending on odd/even effects of the alkane chain length.[7,55] The average well depth of 6.75 meV for $He-CH_3-Si(111)$ is thus in excellent agreement with that reported for other, similar systems.

Once the well depths and decay rates have been determined, an expression for the Debye–Waller exponent can be used to calculate the effective surface Debye temperature θ_D. The effective surface Debye temperature for molecular adlayers describes the dynamic motion normal to the surface and thus describes the stiffness of the layer. For the specular scattering geometry, and assuming that T_S is of the order of the Debye temperature, the decay rate can be written as[44]

$$\sigma_{00} = \frac{24m(E_i \cos^2(\theta_i) + D)}{M_{\text{eff}} k_B \theta_D^2}, \tag{11}$$

where m is the particle mass, M_{eff} is the effective surface mass, and k_B is Boltzmann's constant. Recently, the surface dynamics of silica glass were measured by HAS and the effective surface mass was determined to be 18 amu.[56] This effective mass roughly matches the hydroxyl termination of the silica surface giving us confidence in assuming the effective mass of the $CH_3-Si(111)$ surface to be 15 amu. The surface Debye temperature θ_D was determined to be 983 ± 31 K (683 cm^{-1}) using the experimentally determined well depth of 7.5 ± 2.6 meV and assuming $M_{\text{eff}} = 15$ amu for CH_3. Likewise, $\theta_D = 824 \pm 40$ K (573 cm^{-1}) was calculated by using $D_D = 6.0 \pm 3.9$ meV and $M_{\text{eff}} = 18$ amu for $CD_3-Si(111)$. The uncertainty in the Debye temperature calculations results primarily from the imprecision of the experimentally determined well depths. Both terminations should have the same interaction potential with helium, as isotopic substitution does not alter the van der Waals attraction. Taking the average well depth (i.e., $D = 6.75$ meV), the calculated Debye temperature of the methyl-terminated surface decreases slightly to 974 K, while the value for the $CD_3-Si(111)$ surface increases to 832 K (changes of less than 1%).

The Debye temperature for bulk silicon is 645 K and the surface Debye temperature for Si(111) has been estimated to be 476 K.[50] Typically, surfaces have lower Debye temperatures than bulk crystals because of the reduced dimensionality and the decrease in the phonon frequencies at the interface. Moreover, the effective Debye temperatures of a variety of organic adlayers and thin films have been measured and the materials are generally described as soft (i.e., small θ_D).[57,58] In contrast to typical organic films, the ordered benzene rings of a biphenydimethyldithiol film on a gold substrate created an extraordinarily stiff lattice, with an experimentally measured Debye temperature of 1397 K.[59] The rigidity was comparable to in-plane graphite motion ($\theta_D \sim 1600$ K) and has been ascribed to both the stiffness of the benzene ring itself and to the π-π alignment between adjacent rings. Collectively, these results have demonstrated that the effective Debye temperature is sensitive to the local chemical and structural environments.

For the CH_3-terminated surface, θ_D increased by over 300 K relative to bulk Si, suggesting that rigidity is imposed by the presence of higher frequency modes. HREELS measurements showed the energy of the Si–C stretching mode to be about 680 cm^{-1} (980 K),[34,35] which matches the value determined by the HAS experiment. By the selection rules of the specular geometry ($\Delta K = 0$ $Å^{-1}$), the detected helium atoms can only interact with z-polarized modes during the collision. Although a strong momentum mismatch is present between the helium atom and the Si–C vibration, the agreement between the surface Debye temperature and the Si–C vibrational frequency indicates a coupling between helium and the Si–C stretching mode. Given our observation of helium atom interaction with localized molecular modes and not the phonons of the underlying silicon lattice, a consistent explanation of the data is that the displacement field at the surface is dominated by the adsorbate layer vibrations in the perpendicular direction.

Examination of the Debye temperature of the CD_3-terminated Si(111) surface supports the argument advanced above. As expected, the greater mass of $Si-CD_3$ relative to $Si-CH_3$ produces a decrease in the effective Debye temperature. The gas-phase $Si-CH_3$ stretch is 700 cm^{-1} for CH_3SiH_3, which is close to the 683 cm^{-1} frequency observed for the $CH_3-Si(111)$ surface.[49] The gas-phase $Si-CD_3$ stretch in CD_3SiH_3 is 645 cm^{-1}, a difference of 55 cm^{-1} between the isotopologues.[49] When additional mass is added to the silane group by substituting the hydrogens bound to silicon with deuterium (i.e., CD_3SiD_3), the Si–C stretch frequency is further decreased by an additional 81 cm^{-1}, to 619 cm^{-1}. Considering that each surface silicon atom is bound to three other silicon atoms in the lattice, the observed frequency reduction of about 110 cm^{-1} is thus reasonable and comparable to that observed for gas-phase silanes.

The perpendicular MSDs can be explained by accounting for the sharp increase in effective Debye temperature in conjunction with the reduction in surface mass. Comparing methyl-terminated Si(111) to $Si(111)-(7\times7)$, the mass is

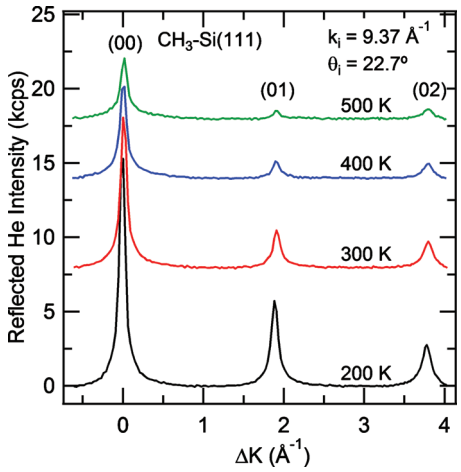

FIG. 6. Thermal attenuation of zero-order, first-order, and second-order diffraction peaks for CH_3–Si(111). The decays are used in the Debye–Waller analysis to calculate the parallel mean-square displacements [Eq. (8)].

reduced by a factor of 1.9, while the ratio of the squared Debye temperatures increases by a factor of ~4. Taking into account the two competing effects, the overall MSD of methyl-terminated Si(111) should be reduced by about a factor of two relative to that of the Si(111)–(7×7) surface, in accord with the observations reported herein. Hence, methylation reduces the perpendicular vibrational motion of the surface relative to bare Si(111).

Finally, we have investigated the mean-square displacements in the surface plane by measuring the thermal attenuation of the first-order and second-order diffraction peaks (Fig. 6). The diffraction patterns are vertically offset for clarity. With experimental values for the perpendicular MSD and for the well depth D from the specular scattering measurements, the parallel MSD can be determined by the use of Eq. (8). The Si–CH_3 bending mode should be the main contributor to the mean-square displacement parallel to the surface. Figure 6 shows the decay of the (01) and (02) diffraction peaks of the CH_3-terminated Si(111) surface at T_S=200, 300, 400, and 500 K, respectively. The data were recorded with k_i=9.37 Å^{-1} at θ_i=22.7°. Three different incident angles (θ_i=22.7°,29.7°,36.2°) were collected for each surface. These angles were chosen so that intensity decays could be obtained for both positive and negative first-order and second-order peaks. The influence of the perpendicular motions was removed from each decay rate, leaving only the parallel contributions, as shown recently for a semicrystalline polymer film.[60] Averaging over the different rates, the parallel mean-square displacements were found to be $(7.1\pm5.1)\times10^{-4}$ Å^2 K^{-1} for CH_3–Si(111) and $(7.2\pm5.3)\times10^{-4}$ Å^2 K^{-1} for CD_3–Si(111) surfaces, respectively.

The calculated parallel thermal motion is an order of magnitude greater than the motion calculated strictly perpendicular to the surface. The perpendicular MSDs were 1.0×10^{-5} and 1.2×10^{-5} Å^2 K^{-1} for CH_3–Si(111) and CD_3–Si(111) surfaces, respectively. The parallel motion is expected to increase more quickly with surface temperature due to the soft bending modes of the methyl groups compared to the stiffer Si–C stretching in the z-direction. Recent theoretical calculations have predicted a coupling of the bending modes with the near-surface phonons of the silicon underlayer, which could potentially contribute to the observed enhancement of the parallel MSDs relative to the perpendicular displacements.[61] For comparison, Scoles and co-workers[51] measured a parallel MSD of 5.0×10^{-4} Å^2 K^{-1} for the methyl-terminated organic crystal. Furthermore, a 21-carbon chain alkanethiol exhibited a parallel MSD of 7.2×10^{-4} Å^2 K^{-1}.[7] This order of magnitude for the parallel thermal motion thus seems to describe a variety of methyl surface groups.

The vibrational dynamics of bare silicon surfaces are dominated by surface phonons, while soft molecular modes are the main contributors to the dynamics of interfaces functionalized with organic adlayers. Our results have revealed that the thermal motion of the methyl-terminated surface is similar to a rigid semiconductor in the normal direction and is like that of an alkanethiol SAM in the surface plane. The addition of a single carbon alkyl group is thus sufficient to drive the transition from phonon-dominated dynamics to a regime in which the motion is governed by local molecular modes.

IV. CONCLUSION

Helium atom diffraction has provided information on the surface structure, gas-surface interaction potential, and vibrational dynamics of CH_3- and CD_3-terminated Si(111) surfaces. Methylation of the silicon surface generates large domains while preserving the native structure of the underlayer. Using the angular dependence of the temperature-induced specular decay, the He-surface potential well depths and Debye temperatures have been estimated for both surfaces. The thermal motions of the alkyl groups both perpendicular and parallel to the surface have been quantified by determination of the mean-square displacements. Elastic scattering decay occurs primarily through coupling between helium atoms and Si–CH_3 molecular vibrations upon collision. In summary, we have probed the vibrational dynamics of this technologically relevant surface, providing complementary information to the well-studied static properties of these interfaces.

ACKNOWLEDGMENTS

This work was supported at the University of Chicago by the Air Force Office of Scientific Research and the UChicago NSF Materials Research Science and Engineering Center and at Caltech by NSF Grant No. CHE-0911682.

[1] J. D. Swalen, D. L. Allara, J. D. Andrade, E. A. Chandross, S. Garoff, J. Israelachvili, T. J. McCarthy, R. Murray, R. F. Pease, J. F. Rabolt, K. J. Wynne, and H. Yu, Langmuir **3**, 932 (1987).
[2] A. Ulman, Chem. Rev. (Washington, D.C.) **96**, 1533 (1996).
[3] A. Bansal, X. L. Li, S. I. Yi, W. H. Weinberg, and N. S. Lewis, J. Phys. Chem. B **105**, 10266 (2001).
[4] S. F. Bent, Surf. Sci. **500**, 879 (2002).
[5] D. H. Wei, C. L. Gao, K. Zakeri, and M. Przybylski, Phys. Rev. Lett. **103**, 225504 (2009).
[6] L. H. Dubois and R. G. Nuzzo, Annu. Rev. Phys. Chem. **43**, 437 (1992).
[7] N. Camillone, C. E. D. Chidsey, G. Y. Liu, T. M. Putvinski, and G. Scoles, J. Chem. Phys. **94**, 8493 (1991).
[8] G. E. Poirier, Chem. Rev. (Washington, D.C.) **97**, 1117 (1997).
[9] F. Schreiber, A. Eberhardt, T. Y. B. Leung, P. Schwartz, S. M. Wetterer,

D. J. Lavrich, L. Berman, P. Fenter, P. Eisenberger, and G. Scoles, Phys. Rev. B **57**, 12476 (1998).
[10] S. B. Darling, A. M. Rosenbaum, and S. J. Sibener, Surf. Sci. **478**, L313 (2001).
[11] B. S. Day and J. R. Morris, J. Phys. Chem. B **107**, 7120 (2003).
[12] N. Isa, K. D. Gibson, T. Yan, W. Hase, and S. J. Sibener, J. Chem. Phys. **120**, 2417 (2004).
[13] A. W. Rosenbaum, M. A. Freedman, S. B. Darling, I. Popova, and S. J. Sibener, J. Chem. Phys. **120**, 3880 (2004).
[14] J. A. Carter, Z. H. Wang, and D. D. Dlott, Acc. Chem. Res. **42**, 1343 (2009).
[15] M. Kind and C. Woll, Prog. Surf. Sci. **84**, 230 (2009).
[16] A. Kumar, N. L. Abbott, E. Kim, H. A. Biebuyck, and G. M. Whitesides, Acc. Chem. Res. **28**, 219 (1995).
[17] M. Mrksich, Cell. Mol. Life Sci. **54**, 653 (1998).
[18] J. C. Love, L. A. Estroff, J. K. Kriebel, R. G. Nuzzo, and G. M. Whitesides, Chem. Rev. (Washington, D.C.) **105**, 1103 (2005).
[19] Z. A. Gurard-Levin and M. Mrksich, Annu. Rev. Anal. Chem. **1**, 767 (2008).
[20] M. R. Linford and C. E. D. Chidsey, J. Am. Chem. Soc. **115**, 12631 (1993).
[21] G. P. Lopinski, D. D. M. Wayner, and R. A. Wolkow, Nature (London) **406**, 48 (2000).
[22] P. T. Hurley, E. J. Nemanick, B. S. Brunschwig, and N. S. Lewis, J. Am. Chem. Soc. **128**, 9990 (2006).
[23] M. Z. Hossain, H. S. Kato, and M. Kawai, J. Am. Chem. Soc. **129**, 3328 (2007).
[24] P. Dumas, Y. J. Chabal, R. Gunther, A. T. Ibrahimi, and Y. Petroff, Prog. Surf. Sci. **48**, 313 (1995).
[25] J. W. P. Hsu, C. C. Bahr, A. V. Felde, S. W. Downey, G. S. Higashi, and M. J. Cardillo, J. Appl. Phys. **71**, 4983 (1992).
[26] A. Bansal, X. L. Li, I. Lauermann, N. S. Lewis, S. I. Yi, and W. H. Weinberg, J. Am. Chem. Soc. **118**, 7225 (1996).
[27] W. J. Royea, A. Juang, and N. S. Lewis, Appl. Phys. Lett. **77**, 1988 (2000).
[28] S. Maldonado, D. Knapp, and N. S. Lewis, J. Am. Chem. Soc. **130**, 3300 (2008).
[29] S. Maldonado and N. S. Lewis, J. Electrochem. Soc. **156**, H123 (2009).
[30] H. B. Yu, L. J. Webb, R. S. Ries, S. D. Solares, W. A. Goddard, J. R. Heath, and N. S. Lewis, J. Phys. Chem. B **109**, 671 (2005).
[31] L. J. Webb and N. S. Lewis, J. Phys. Chem. B **107**, 5404 (2003).
[32] B. Jaeckel, R. Hunger, L. J. Webb, W. Jaegermann, and N. S. Lewis, J. Phys. Chem. C **111**, 18204 (2007).
[33] R. Hunger, R. Fritsche, B. Jaeckel, W. Jaegermann, L. J. Webb, and N. S. Lewis, Phys. Rev. B **72**, 045317 (2005).
[34] T. Yamada, M. Kawai, A. Wawro, S. Suto, and A. Kasuya, J. Chem. Phys. **121**, 10660 (2004).
[35] T. Yamada, T. Inoue, K. Yamada, N. Takano, T. Osaka, H. Harada, K. Nishiyama, and I. Taniguchi, J. Am. Chem. Soc. **125**, 8039 (2003).
[36] L. J. Webb, S. Rivillon, D. J. Michalak, Y. J. Chabal, and N. S. Lewis, J. Phys. Chem. B **110**, 7349 (2006).
[37] H. B. Yu, L. J. Webb, J. R. Heath, and N. S. Lewis, Appl. Phys. Lett. **88**, 252111 (2006).
[38] G. S. Higashi, Y. J. Chabal, G. W. Trucks, and K. Raghavachari, Appl. Phys. Lett. **56**, 656 (1990).
[39] E. J. Nemanick, P. T. Hurley, B. S. Brunschwig, and N. S. Lewis, J. Phys. Chem. B **110**, 14800 (2006).
[40] B. Gans, P. A. Knipp, D. D. Koleske, and S. J. Sibener, Surf. Sci. **264**, 81 (1992).
[41] B. Poelsema and G. Comsa, *Scattering of Thermal Energy Atoms from Disordered Surfaces* (Springer-Verlag, Berlin, 1989).
[42] G. Comsa, Surf. Sci. **81**, 57 (1979).
[43] J. Lapujoulade, Y. Lejay, and G. Armand, Surf. Sci. **95**, 107 (1980).
[44] *Atomic and Molecular Beam Methods*, edited by G. Scoles (Oxford University Press, Oxford, 1992).
[45] D. Farias and K. H. Rieder, Rep. Prog. Phys. **61**, 1575 (1998).
[46] J. L. Beeby, J. Phys. C **4**, L359 (1971).
[47] G. Bracco, M. D. Ward, and G. Scoles, J. Chem. Phys. **118**, 8405 (2003).
[48] G. Pelz, P. Mittler, K. M. T. Yamada, and G. Winnewisser, J. Mol. Spectrosc. **156**, 390 (1992).
[49] A. J. F. Clark and J. E. Drake, Can. J. Spectrosc. **22**, 79 (1977).
[50] J. S. Ha and E. F. Greene, J. Chem. Phys. **91**, 571 (1989).
[51] G. Bracco, J. Acker, M. D. Ward, and G. Scoles, Langmuir **18**, 5551 (2002).
[52] T. Y. B. Leung, P. Schwartz, G. Scoles, F. Schreiber, and A. Ulman, Surf. Sci. **458**, 34 (2000).
[53] *Helium Atom Scattering from Surfaces*, edited by E. Hulpke (Springer, Berlin, 1992).
[54] J. R. Buckland and W. Allison, J. Chem. Phys. **112**, 970 (2000).
[55] G. Bracco and G. Scoles, J. Chem. Phys. **119**, 6277 (2003).
[56] W. Steurer, A. Apfolter, M. Koch, W. E. Ernst, E. Sondergard, J. R. Manson, and B. Holst, Phys. Rev. B **78**, 045427 (2008).
[57] J. J. Hernández, J. A. Li, J. Baker, S. A. Safron, and J. G. Skofronick, J. Vac. Sci. Technol. A **14**, 1788 (1996).
[58] C. N. Borca, S. Adenwalla, J. W. Choi, P. T. Sprunger, S. Ducharme, L. Robertson, S. P. Palto, J. L. Liu, M. Poulsen, V. M. Fridkin, H. You, and P. A. Dowben, Phys. Rev. Lett. **83**, 4562 (1999).
[59] D. Q. Feng, P. A. Dowben, R. Rajesh, and J. Redepenning, Appl. Phys. Lett. **87**, 181918 (2005).
[60] J. S. Becker, R. D. Brown, D. R. Killelea, H. Yuan, and S. J. Sibener, "Comparative surface dynamics of amorphous and semicrystalline polymer films," Proc. Natl. Acad. Sci. U.S.A. (in press).
[61] G. A. Ferguson and K. Raghavachari, J. Chem. Phys. **125**, 154708 (2006).